

UI-AGILE: Advancing GUI Agents with Effective Reinforcement Learning and Precise Inference-Time Grounding

Shuquan Lian¹, Yuhang Wu¹, Jia Ma¹, Yifan Ding¹, Zihan Song¹, Bingqi Chen¹, Xiawu Zheng¹, Hui Li¹

¹Key Laboratory of Multimedia Trusted Perception and Efficient Computing Ministry of Education of China, Xiamen University

15420202202203@stu.xmu.edu.cn

Abstract

The emergence of Multimodal Large Language Models (MLLMs) has driven significant advances in Graphical User Interface (GUI) agent capabilities. Nevertheless, existing GUI agent training and inference techniques still suffer from a dilemma for reasoning designs, ineffective reward, and visual noise. To address these issues, we introduce UI-AGILE for enhancing GUI agents at both training and inference. For training, we propose a suite of improvements to the Supervised Fine-Tuning (SFT) process: 1) a continuous reward function to incentivize high-precision grounding; 2) a “Simple Thinking” reward to balance planning with speed and grounding accuracy; and 3) a cropping-based resampling strategy to mitigate the sparse reward problem and improve learning on complex tasks. For inference, we present decomposed grounding with selection to dramatically improve grounding accuracy on high-resolution displays by breaking the image into smaller, manageable parts. Experiments show that UI-AGILE achieves the state-of-the-art grounding performance on two benchmarks ScreenSpot-Pro and ScreenSpot-v2 while it also exhibits strong general agent capabilities. For instance, using both our training and inference enhancement methods brings 23% grounding accuracy improvement over the best baseline on ScreenSpot-Pro. We provide the code in <https://github.com/KDEGroup/UI-AGILE>.

1 Introduction

Driven by the growing capabilities of Multimodal Large Language Models (MLLMs) in image understanding (Bai et al. 2025), Graphical User Interface (GUI) agents, which execute tasks by understanding screenshots and user instructions, are advancing rapidly (Zhang et al. 2025).

Prior methods for GUI agents mostly rely on Supervised Fine-Tuning (SFT), requiring a large amount of human-annotated or synthesized data for teaching agents how to plan its actions and grounding (Gou et al. 2025; Wu et al. 2025; Lin et al. 2025). Recently, Reinforcement Fine-Tuning (RFT) has been proposed to enhance GUI agents (Lu et al. 2025; Luo et al. 2025), and achieves considerable improvements compared to previous approaches.

Despite the significant momentum of GUI agent techniques, their practical application is hindered by several limitations in both training and inference stages:

- **P1: A Dilemma for Reasoning Designs:** An elaborate reasoning process not only degrades grounding accuracy

but also increases inference latency, while a “No Thinking” approach exhibits low accuracy for predicting non-grounding action types (Shen et al. 2025).

- **P2: Ineffective Reward:** Agents often get stuck on complex interfaces and receive no effective learning signal (i.e., sparse reward). Besides, simple binary feedback (correct/incorrect), a design used by many existing methods (Lu et al. 2025; Luo et al. 2025) may fail to endow agents with the ability to perform precise localization.
- **P3: Visual Noise:** Even well-trained agents frequently struggle to cope with high-resolution screens, as irrelevant visual noise degrades their grounding accuracy.

To address the above problems, we propose UI-AGILE, a framework aiming at improving both the RFT and the inference stages of GUI agents. Its contributions are as follows:

- To overcome **P1**, UI-AGILE applies a “Simple Thinking” strategy that employs reasoning through thoughts with appropriate lengths. “Simple Thinking” effectively balances the improvement of both the core grounding task and the prediction of non-grounding action types.
- To tackle **P2**, UI-AGILE harnesses a design of continuous grounding reward for the RFT stage to incentivize more precise localization to the target’s center. Furthermore, UI-AGILE employs cropping-based resampling to dynamically adjust the difficulty of training samples to avoid ineffective training with zero reward.
- To solve **P3**, UI-AGILE uses a visual noise reduction method termed decomposed grounding with selection. It decomposes a high-resolution screenshot into multiple sub-images, generates candidate elements on each, and finally uses a Vision-Language Model (VLM) to “adjudicate” the best match. This approach significantly improves the agent’s grounding accuracy on high-resolution displays during inference.

Extensive experiments validate the effectiveness of our methods. Trained on about only 9k samples for just 2 epochs, UI-AGILE shows superior performance, while also showcasing strong general agent capabilities. Furthermore, our inference method can act as a plug-and-play enhancement for a wide range of existing agents, improving the accuracy of some existing open-source models.

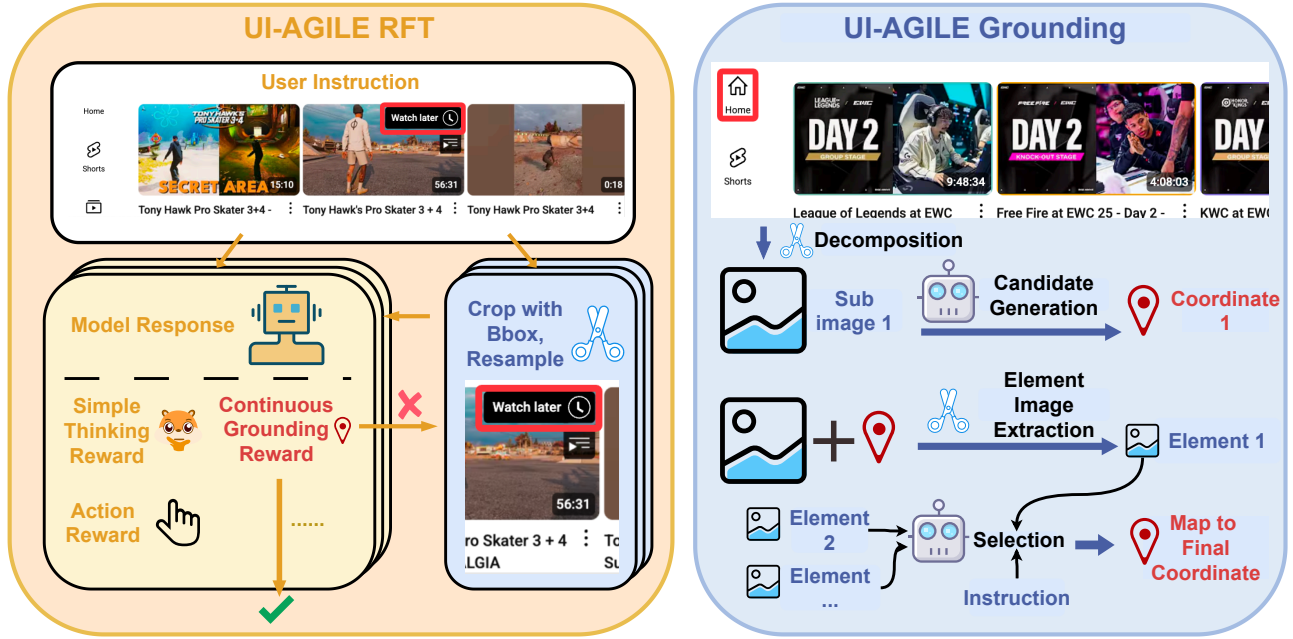


Figure 1: An overview of UI-AGILE. (1) Left: The training stage is enhanced with our three core contributions: “Simple Thinking”, continuous grounding reward and cropping-based resampling. Continuous grounding reward being zero would result in crop-based resampling. (2) Right: The inference stage uses our proposed decomposed grounding with selection.

2 Related Work

Reinforcement Learning (RL) for Large Models Recently, reinforcement learning (RL) for training large models has gained significant momentum. The focus has shifted from traditional policy optimization algorithms like PPO (Schulman et al. 2017), towards alignment-centric methods such as DPO (Rafailov et al. 2023), and more recent rule-based algorithms like GRPO (Shao et al. 2024). These algorithms have achieved remarkable success in enhancing the reasoning capabilities of large models on complex tasks, with models like OpenAI O1 (Jaech et al. 2024) and DeepSeek-R1 (DeepSeek-AI et al. 2025). The efficacy of these approaches promotes their rapid extension into the multimodal domain (Chen et al. 2025; Chen, Luo, and Li 2025; Liu et al. 2025b; Peng et al. 2025; Meng et al. 2025).

GUI Agents The field of GUI agents has evolved rapidly (Wang et al. 2024; Li and Huang 2025). Following early works like CogAgent (Hong et al. 2024) and SeeClick (Cheng et al. 2024), most studies rely on SFT to operate directly on visual inputs. Show-UI (Lin et al. 2025) innovates on visual processing efficiency. OS-Atlas (Wu et al. 2025), UGround (Gou et al. 2025) and Aria-UI (Yang et al. 2024) propose novel, large-scale pipelines to collect and synthesize millions of GUI agent trajectories, significantly improving model generalization. Aguis (Xu et al. 2024) introduced a two-stage training process that explicitly uses VLM-generated Chain-of-Thought (CoT) data to teach planning and reasoning. JEDI (Xie et al. 2025) constructs a refusal part by mismatching existing instructions with unrelated screenshots. Standing out in complexity and

scale, UI-TARS (Qin et al. 2025) utilizes the largest dataset and the most intricate training pipeline, which involves SFT and DPO on human annotated CoT data to improve performance. This data-intensive scaling has motivated a shift towards more effective RL paradigms, first explored by UI-R1 (Lu et al. 2025) and GUI-R1 (Luo et al. 2025). InfiGUI-R1 (Liu et al. 2025a) employs Spatial Reasoning Distillation and RL to enhance planning and error recovery capabilities. GUI-G1 (Zhou et al. 2025) leverages Hit-based reward and IoU-based reward for improving GUI agents.

3 Our Framework UI-AGILE

Fig. 1 provides an overview of UI-AGILE, which aims at improving both training and inference stages of GUI agents.

At training time, the model generates multiple responses from an image and instruction, which are evaluated by reward functions, including “Simple Thinking” reward for efficient reasoning (Sec. 3.1) and continuous grounding reward (Sec. 3.2) for precise localization. If a training sample proves too difficult (i.e., receive a grounding reward of zero for all generated responses), the image will be cropped to simplify the task, and the model resamples new responses from this modified input.

At inference time, UI-AGILE applies decomposed grounding with selection (Sec. 3.4) to enhance grounding on the high-resolution displays common in modern applications, making GUI agents more practical for real-world use.

3.1 “Simple Thinking” for Reconciling the Reasoning Dilemma (P1)

Lu et al. (2025) posit that excessive reasoning is not essen-

tial for GUI grounding and can even be detrimental. However, *the complete role of GUI agents extends beyond mere grounding*, and deciding next action (e.g., click or type) inherently demands a foundational level of reasoning.

To reconcile the dilemma of whether to apply reasoning for enhancing action-type prediction or discard excessive reasoning to avoid ineffective grounding, we propose a ‘‘Simple Thinking’’ strategy. It encourages thoughts with an appropriate length, operationalized through a specialized reward function. It also reduces training and inference costs, a practical consideration for real-world deployment.

The reward R_{think} for the thought process is defined as:

$$R_{think} = I(R_{grounding} > 0) \cdot (R_{length}(L) + R_{bonus}) \quad (1)$$

$$R_{length}(L) = \begin{cases} 1.0 & \text{if } l_{ideal.start} < L \leq l_{ideal.end} \\ \frac{1}{2} \left(1 - \cos \left(\pi \frac{L - l_{min}}{l_{ideal.start} - l_{min}} \right) \right) & \text{if } l_{min} < L \leq l_{ideal.start} \\ \frac{1}{2} \left(1 + \cos \left(\pi \frac{L - l_{ideal.end}}{l_{max} - l_{ideal.end}} \right) \right) & \text{if } l_{ideal.end} < L < l_{max} \\ 0 & \text{otherwise} \end{cases} \quad (2)$$

where:

- $I(R_{grounding} > 0)$ is an indicator function that grants reward only when the grounding reward $R_{grounding} > 0$, linking reasoning to effective outcomes.
- $R_{length}(L)$ is a non-linear reward based on the reasoning length L . $l_{ideal.start}$ and $l_{ideal.end}$ define an ideal range of reasoning length, where reward is 1. The reward will be zero if the reasoning length exceeds l_{min} or l_{max} .
- R_{bonus} is a fixed bonus for syntactically complete thoughts (e.g., ending with proper punctuation), encouraging structured reasoning.

‘‘Simple Thinking’’ defines an ideal range where the reward is maximized, encouraging thoughts that are neither too brief (‘‘under-thinking’’) nor too verbose (‘‘over-thinking’’). Outside this ideal range, it uses the cosine function for smooth degradation down to a reward of zero at the absolute bounds. This smooth, non-linear penalty provides a more stable learning signal for RL than a hard cliff. Furthermore, the additional bonus for syntactically complete thoughts discourages incomplete reasoning, thereby ensuring better training stability.

3.2 Continuous Grounding Reward for Precise Localization (P2)

Unlike general visual grounding tasks which compute the IoU between the predicted bounding box and the ground truth box, GUI agents usually predict a click point and receive a simple binary reward in rule-based RFT (Lu et al. 2025; Luo et al. 2025): a reward of 1 for a correct prediction (e.g., inside the ground truth box) and 0 otherwise.

However, this binary reward is insufficient for high-precision control, as it equally rewards clicks on an element’s edge and at its center. This non-discriminatory feedback misguides the model to learn an element’s boundaries rather than its semantic core.

To resolve this issue, we introduce a continuous grounding reward. Instead of a binary outcome, the continuous reward is calculated as a function of the distance from the predicted point to the center of the ground-truth bounding box:

$$R(x, y) = \begin{cases} 1 + \exp(-4 \cdot d_{norm}^2) & \text{if } (x, y) \in \text{BBox} \\ 0 & \text{otherwise} \end{cases} \quad (3)$$

where:

- $R(x, y)$ is the reward score for the predicted coordinate.
- (x, y) is the coordinate predicted by the agent.
- BBox is the ground-truth bounding box, defined by its top-left (x_1, y_1) and bottom-right (x_2, y_2) corners.
- d_{norm} is the Chebyshev distance (or L_∞ norm) of the point from the center of the bounding box, normalized by the box’s dimensions. It is calculated as:

$$d_{norm} = \max \left(\frac{|x - c_x|}{w_h}, \frac{|y - c_y|}{h_h} \right) \quad (4)$$

Here, $(c_x, c_y) = (\frac{x_1+x_2}{2}, \frac{y_1+y_2}{2})$ represents the center of the bounding box, and $(w_h, h_h) = (\frac{x_2-x_1}{2}, \frac{y_2-y_1}{2})$ are its half-width and half-height, respectively.

We employ the Chebyshev distance instead of the Euclidean distance because the reward contours generated by the Chebyshev distance are squares, which geometrically align with the rectangular shape of GUI bounding boxes. This alignment provides a more logical and consistent reward landscape, strongly incentivizing the agent to minimize its deviation along both axes to achieve a high reward.

3.3 Cropping-Based Resampling for Sparse Reward Mitigation (P2)

During GRPO training, GUI agents often face the sparse reward challenge, particularly on complex tasks. When the model fails to place its prediction within the correct bounding box for a given screenshot over all generations, it receives reward of 0. The lack of positive signals can lead to training stagnation, and difficult samples cannot contribute to model improvement.

Inspired by curriculum learning (Bengio et al. 2009), which presents training examples in an easy-to-hard progression, we propose Cropping-based Resampling. This method acts as a dynamic difficulty adjustment mechanism: if a sample yields zero reward over all generations, we deem it too difficult and reduce its complexity by cropping the screenshot. The resulting smaller crop is guaranteed to fully contain the ground-truth bounding box.

A naive implementation is to center the ground-truth bounding box (bbox) in the new cropping, but it may fail to endow the model with the capability to perform robust localization: the model would learn a trivial shortcut, such as developing a bias for predicting the image center. We opt to employ a scanning approach as illustrated in Alg. 1, ensuring that the cropped image fully contains the ground-truth bounding box. It firstly determines the size of cropping based on a predefined ratio (lines 1-2). Then, the horizontal stride $step_x$ is set to the difference between the cropping width and the bounding box width, while the vertical

Algorithm 1: Cropping-Based Resampling

Input: $Image, Bbox, scalingFactor$
Output: $Set(Image_{crop}, Bbox_{crop})$

- 1: $(w_o, h_o) \leftarrow GetWidthAndHeight(Image)$
- 2: $(w_{crop}, h_{crop}) \leftarrow (w_o \times f, h_o \times f)$
- 3: $(w_b, h_b) \leftarrow (Bbox[2] - Bbox[0], Bbox[3] - Bbox[1])$
- 4: $step_x \leftarrow w_{crop} - w_b$
- 5: $step_y \leftarrow h_{crop} - h_b$
- 6: $T \leftarrow \emptyset$
- 7: **for** $xcrop_{min}$ from 0 to w_o $step=step_x$ **do**
- 8: $xcrop_{max} \leftarrow \min(xcrop_{min} + w_{crop}, w_o)$
- 9: **for** $ycrop_{min}$ from 0 to h_o $step=step_y$ **do**
- 10: $ycrop_{min} \leftarrow \min(ycrop_{min} + h_{crop}, h_o)$
- 11: $Coord_{crop} \leftarrow [xcrop_{min},$
 $ycrop_{min}, xcrop_{max}, ycrop_{max}]$
- 12: **if** $Bbox$ is contained within $Coord_{crop}$ **then**
- 13: $Image_{crop} \leftarrow Crop(Image, Coord_{crop})$
- 14: $Bbox_{crop} \leftarrow Bbox - Coord_{crop}$
- 15: $Set \leftarrow Set \cup (Image_{crop}, Bbox_{crop})$
- 16: **end if**
- 17: **end for**
- 18: **end for**
- 19: **return** Set

stride $step_y$ is set to the difference between their respective heights (lines 3-5). After that, it iterates through all possible cropping windows from left-to-right and top-to-bottom across the original screenshot with the horizontal stride and the vertical stride (lines 7-18). The first window that fully contains the ground-truth bbox is selected as the new, re-sampled input (lines 12-16). Fig. 2 illustrates how our scanning approach identifies valid cropping windows that fully contain the ground-truth bounding box.

Cropping-based resampling dynamically simplifies difficult samples to ensure that they are learnable, allowing the model to leverage more data in fewer epochs, yielding superior results within a similar amount of training time.

3.4 Decomposed Grounding with Selection for Visual Noise Reduction (P3)

Modern electronic devices feature high-resolution displays (e.g., 3840x2160), which, when converted into tokens for a VLM, can result in an overwhelmingly long sequence (e.g., over 10,000 tokens). We hypothesize that a significant portion of these tokens represent irrelevant background information, i.e., the visual noise issue **P1** mentioned in Sec. 1.

To validate this hypothesis, we conduct a preliminary experiment on ScreenSpot-Pro (Li et al. 2025). We apply the cropping method in Sec. 3.3, but for the purpose of creating a controlled test environment. For each original screenshot, we crop it to 1024x1024, ensuring the ground-truth bounding box is contained within the frame. On this new dataset, the grounding accuracy of UGround-V1-7B (Gou et al. 2025) shows a significant improvement from 31.6 to 56.0, verifying our hypothesis.

It is straightforward to consider applying the cropping-based method to alleviate the visual noise. However, during inference, the location of the ground-truth bounding box is unknown, making such oracle-based cropping impossi-

ble. To overcome this challenge, we propose a multi-stage decomposed grounding with selection method as shown in the right part of Fig. 1. It reduces visual noise by cropping an image into several sub-images and predicts the coordinate individually, while trying to maintain full ground-truth bounding box area. The detailed process is as follows:

1. **Decomposition:** The input screenshot is first divided into several overlapping sub-images, breaking down the high-resolution screen into smaller, more manageable regions.
2. **Candidate Generation:** The GUI agent performs grounding independently on each sub-image and predicts a coordinate for the sub-image. Then, we use the predicted coordinates of sub-images belonging to a screenshot as the candidate coordinates for the screenshot.
3. **Element Image Extraction:** For each candidate point, we extract the corresponding element image by cropping a bounding box centered on the candidate point from the sub-image.
4. **Selection:** We use a VLM to score each candidate image based on a direct “Yes/No” question asking if it matches the user’s instruction (see Appendix A for the prompt). The output logit for “Yes” serves as the relevance score. The coordinates of the highest-scoring candidate are then remapped to the original screenshot. This QA-based process enables deeper contextual prediction.

This process directly benefits from the continuous reward function, as it trains the model to predict points closer to the center of target elements, leading to higher-quality extracted images and thus a more accurate final selection.

Analysis of Inference Cost. We analyze the inference latency of using decomposed grounding with selection by breaking it down into three primary stages: prefilling, decoding and selection stage.

Counter-intuitively, our approach can *theoretically accelerate the computationally-heavy prefilling stage*. Recall that the self-attention mechanism has a quadratic time complexity $\mathcal{O}(n^2)$ concerning the input sequence length n (Vaswani et al. 2017). By splitting a single large image with n tokens into 4 sub-images (each with roughly $n/4$ tokens), the total computational cost for attention scales proportionally to $4 \times (\frac{n}{4})^2 = \frac{n^2}{4}$, suggesting a theoretical speedup. Such cost reduction far outweighs the slightly increased overhead of repeatedly processing the text prompt for each sub-image.

While the decoding process runs for each sub-image, the small number of output tokens (compared to image tokens) per run ensures that the cumulative decoding cost will not increase much.

Finally, the VLM-based selection stage is computationally inexpensive. The input element images are very small, and the process only requires a single forward pass to acquire the logits for a “Yes/No” answer.

Overall, the cost of applying decomposed grounding with selection is low. In addition to the above analysis, we provide results on actual running time in Sec. 4.5. Crucially, we believe this overhead could be eliminated or even reversed with future optimizations in inference engines tailored for this “many small requests” workload.

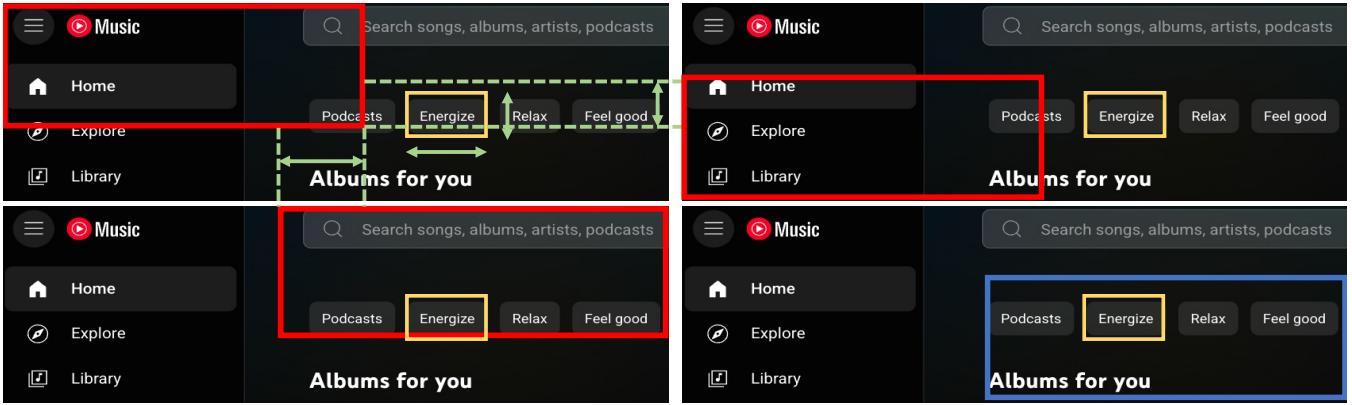


Figure 2: An example of cropping-based resampling. Yellow bounding boxes are the ground truth, red bounding boxes are invalid cropping, and blue bounding boxes are valid cropping. Green arrows show that the overlap of cropping windows is equivalent to the width or height of the ground-truth bounding box.

4 Experiment

4.1 Implementation Details

Data. We collect data from multiple open-source datasets, including UI-R1 (Lu et al. 2025), GUI-R1 (Luo et al. 2025), Aguis (Xu et al. 2024) and Grounding-R1 (Yang et al. 2025). We filter them using OmniParser (Wan et al. 2024) following Grounding-R1 (Yang et al. 2025). We randomly sample about 9k examples to train UI-AGILE.

Details of Environment, Implementation and Default Hyperparameters. Due to space limit, we include the details of environment, implementation and default hyperparameters in Appendix A.

4.2 Grounding Capability Evaluation

We evaluate the grounding ability on ScreenSpot-v2 (Wu et al. 2025) and ScreenSpot-Pro (Li et al. 2025). ScreenSpot-v2 is a corrected version of the original ScreenSpot (Cheng et al. 2024), providing evaluation of GUI grounding capability across mobile, desktop, and web platforms. ScreenSpot-Pro focuses on high-resolution professional environments, featuring expert-annotated tasks spanning 23 applications, five industries, and three operating systems. Since the images in ScreenSpot-v2 are already pre-cropped while those in ScreenSpot-Pro are full, uncropped displays, we evaluate our decomposed grounding with selection method exclusively on ScreenSpot-Pro.

Effectiveness of our inference enhancement. As shown in Tab. 1, decomposed grounding with selection shows significant improvements on ScreenSpot-Pro. It provides a universal and substantial performance boost across all tested models, regardless of their original training paradigm (SFT or RFT). For instance, it elevates the average score of OS-Atlas-7B from 18.9 to 33.1 (+75.1%), and boosts Aguis-7B from 20.4 to 36.5 (+78.9%). The consistent improvement proves the effectiveness of decomposed grounding with selection and its high applicability as a plug-and-play inference enhancement.

Effectiveness of our training enhancement. Besides, Tab. 1 shows that UI-AGILE-3B and UI-AGILE-7B models, even without decomposed grounding, establish a new state-of-the-art among 3B and 7B models on ScreenSpot-Pro. Trained on only 9K examples with 2 epochs, they (37.9 for 3B and 44.0 for 7B) surpass other RFT-based models like UI-R1-E (33.5), InfiGUI-R1-3B and GUI-R1-7B (32.1). UI-AGILE-7B even outperforms the much larger model UI-TARS-72B (38.1) trained on approximately 50 billion tokens. On the ScreenSpot-v2 benchmark (Tab. 2), our UI-AGILE-7B also achieves state-of-the-art grounding accuracy with an average score of 92.1. The above results demonstrate the effectiveness of our proposed “Simple Thinking” reward, continuous grounding reward, and cropping-based resampling for improving the training of GUI agents.

Overall, as shown in Tab. 1, using both our training and inference enhancements (UI-AGILE-7B + Decomposed Grounding) brings 23% grounding accuracy improvement over the best baseline (JEDI-7B) on ScreenSpot-Pro.

4.3 Agent Capability Evaluation

In addition to grounding-specific benchmarks, we also evaluate UI-AGILE-3B and UI-AGILE-7B on AndroidControl (Li et al. 2024) to assess its general agent capabilities.

Following the evaluation setting of OS-Atlas (Wu et al. 2025), we use three metrics: action type prediction accuracy (Type), grounding accuracy (GR), and the overall step success rate (SR). Type accuracy measures the exact match for the predicted action (e.g., click or scroll). For GR, a prediction is considered successful if it falls within a 14% screen-width radius of the ground-truth coordinate. The most holistic metric, SR, deems a step successful only if both the action type and all its associated arguments (e.g., coordinates for a click, direction for a scroll, or text for an input) are correct.

Following OS-Atlas, we use 7,708 examples for a fair comparison, while some works (e.g., Aguis (Xu et al. 2024) and UGround (Gou et al. 2025)) randomly sample 500 action steps for testing. The evaluation is conducted under two distinct settings. In AndroidControl-Low, the agent receives

Model	Examples	Epochs	Dev		Creative		CAD		Scientific		Office		OS		Avg	pass@4
			Text	Icon												
Supervised Fine-tuning																
CogAgent-18B	222M	-	14.9	0.7	9.6	0.0	7.1	3.1	22.2	1.8	13.0	0.0	5.6	0.0	7.7	-
Aria-UI	16.6M	-	16.2	0.0	23.7	2.1	7.6	1.6	27.1	6.4	20.3	1.9	4.7	0.0	11.3	-
ShowUI-2B	256K	-	16.9	1.4	9.1	0.0	2.5	0.0	13.2	7.3	15.3	7.5	10.3	2.2	7.7	-
JEDI-3B	4M	-	61.0	13.8	53.5	8.4	27.4	9.4	54.2	18.2	64.4	32.1	38.3	9.0	36.1	-
JEDI-7B	4M	-	42.9	11.0	50.0	<u>11.9</u>	38.0	14.1	72.9	25.5	<u>75.1</u>	47.2	33.6	16.9	39.5	-
OS-Atlas-7B	13M	-	33.8	1.4	30.8	3.5	12.2	3.1	33.3	9.1	33.3	9.4	26.2	3.4	18.9	-
+Decomposed Grounding	-	-	49.4	5.5	52.0	5.6	26.4	6.3	54.9	18.2	57.6	18.9	49.5	9.0	33.1	42.1
Aguvis-7B	1M	1	30.5	0.7	28.8	2.8	14.7	1.6	45.8	8.2	38.4	11.3	30.8	2.3	20.4	-
+Decomposed Grounding	-	-	50.6	11.7	<u>60.1</u>	7.0	31.0	4.7	62.5	20.0	63.3	18.9	45.8	6.7	36.5	44.3
UGround-V1-7B	10M	-	51.3	5.5	48.5	8.3	18.8	1.6	59.7	14.6	59.9	17.0	40.2	7.9	31.6	-
+Decomposed Grounding	-	-	57.8	14.5	49.0	<u>11.9</u>	20.3	7.8	62.5	21.8	67.8	18.9	48.6	14.6	36.6	47.3
UI-TARS-2B	-	-	47.7	4.1	42.9	6.3	17.8	4.7	56.9	17.3	50.3	17.0	21.5	5.6	27.7	-
UI-TARS-7B	-	-	58.4	12.4	50.0	9.1	20.8	9.4	63.9	31.8	63.3	20.8	30.8	16.9	35.7	-
+Decomposed Grounding	-	-	59.7	<u>19.3</u>	54.0	15.4	38.1	12.5	63.2	27.3	71.8	28.3	45.8	<u>21.3</u>	41.9	50.3
UI-TARS-72B	-	-	63.0	17.3	57.1	15.4	18.8	<u>17.2</u>	64.6	20.9	63.3	26.4	42.1	15.7	38.1	-
Zero Shot / Reinforcement Fine-tuning																
InfGUI-R1-3B	32K	-	51.3	12.4	44.9	7.0	33.0	14.1	58.3	20.0	65.5	28.3	43.9	12.4	35.7	-
GUI-G1-3B	17K	1	50.7	10.3	36.6	<u>11.9</u>	39.6	9.4	61.8	<u>30.0</u>	67.2	32.1	32.5	10.6	37.1	-
Qwen2.5-VL-3B	-	-	31.8	4.1	32.8	4.2	24.9	4.7	43.8	12.7	42.4	15.1	17.8	2.2	22.7	-
+Decomposed Grounding	-	-	52.6	8.3	42.9	11.2	25.9	3.1	47.9	10.0	55.9	17.0	46.7	9.0	31.2	38.8
Qwen2.5-VL-7B	-	-	54.5	5.5	24.7	4.2	13.7	3.1	46.5	7.3	50.8	11.3	29.9	10.1	24.5	-
+Decomposed Grounding	-	-	60.4	13.1	33.3	8.4	27.9	6.2	50.0	13.6	63.3	17.0	51.4	16.0	33.3	42.0
GUI-R1-3B	3K	9	40.9	4.8	47.8	2.8	27.9	6.3	65.3	19.1	58.2	18.9	29.0	2.2	30.9	-
+Decomposed Grounding	-	-	63.6	13.1	55.6	4.9	31.5	6.3	61.8	16.4	62.7	20.8	44.9	10.1	37.1	46.0
GUI-R1-7B	3K	9	57.1	8.3	37.9	8.4	28.4	6.3	54.9	10.9	59.9	13.2	41.1	13.5	32.1	-
+Decomposed Grounding	-	-	<u>66.9</u>	15.2	50.0	10.5	32.5	4.7	59.0	13.6	68.4	24.5	60.7	18.0	39.3	48.6
UI-R1-3B	136	8	22.7	4.1	27.3	3.5	11.2	6.3	42.4	11.8	32.2	11.3	13.1	4.5	17.8	-
UI-R1-E	2K	8	46.1	6.9	41.9	4.2	37.1	12.5	56.9	21.8	65.0	26.4	32.7	10.1	33.5	-
+Decomposed Grounding	-	-	63.6	17.2	59.6	10.0	43.7	6.3	66.0	21.8	68.4	<u>43.4</u>	56.1	19.1	43.3	52.6
UI-AGILE-3B	9K	2	53.2	9.0	50.5	8.4	44.2	20.3	62.5	22.7	65.5	22.6	35.5	12.4	37.9	-
+Decomposed Grounding	-	-	<u>66.9</u>	16.6	58.1	<u>11.9</u>	47.2	10.9	<u>66.7</u>	24.5	72.3	34.0	58.9	22.5	<u>45.0</u>	<u>54.4</u>
UI-AGILE-7B	9K	2	64.3	15.2	53.0	9.8	49.2	14.1	72.9	25.5	<u>75.1</u>	30.2	45.8	20.2	44.0	-
+Decomposed Grounding	-	-	79.1	24.1	60.6	11.2	53.3	10.9	66.0	26.4	79.1	39.6	<u>59.8</u>	22.5	48.7	59.2

Table 1: Grounding accuracy on ScreenSpot-Pro. “+Decomposed Grounding” denotes that the model uses our decomposed grounding with selection for enhancing inference. Results marked in bold represent the best performance, and underlined results indicate the second-best performance. The pass@4 metric indicates the success rate where a task is considered solved if the prediction of at least one of the sub-images is correct.

a specific, low-level instruction for each step. In contrast, AndroidControl-High provides the agent with a high-level goal, requiring it to infer the correct action for the current step based on the conversation history and previous actions, thereby testing its multi-step reasoning capability.

As depicted in Tab. 3, UI-AGILE-7B achieves the best performance (SR: 77.6 and 60.6) compared to other RFT models, including UI-R1-E (SR: 71.37 and 35.88), GUI-R1-3B (SR: 64.41 and 46.55) and GUI-R1-7B (SR: 66.52 and 51.67). Notably, the smaller UI-AGILE-3B (SR: 77.4 and 56.9) also surpasses 7B baselines like GUI-R1-7B (SR: 66.5 and 51.7). For Type, a similar trend can be observed.

For GR, UI-AGILE archives the best performance in most cases except that GUI-R1-7B shows higher GR (65.6) in the AndroidControl-High setting. We attribute it to different training philosophies: their prolonged training on a smaller dataset for 9 epochs may foster specialization, whereas our training on a larger, more diverse dataset for 2 epochs prioritizes generalization. This hypothesis is supported by our model’s dominant performance on dedicated grounding benchmarks ScreenSpot-Pro and ScreenSpot-v2.

Overall, the remarkable results on AndroidControl demonstrate that the improvements gained from our methods are not confined to improving grounding capability but

Method	Mobile		Desktop		Web		Avg.
	Text	Icon	Text	Icon	Text	Icon	
SeeClick	78.4	50.7	70.1	29.3	55.2	32.5	55.1
OS-Atlas-4B	87.2	59.7	72.7	46.4	85.9	63.0	71.9
OS-Atlas-7B	95.0	73.3	92.8	64.9	89.6	72.4	83.7
Aguvis-7B	94.9	80.1	95.0	77.9	91.4	69.9	85.6
Qwen2.5-VL-3B	96.1	74.8	87.8	53.0	86.9	70.4	80.7
Qwen2.5-VL-7B	98.4	84.8	88.4	74.7	92.5	77.6	87.5
GUI-R1-3B	98.1	79.0	94.0	66.7	93.3	69.2	85.2
GUI-R1-7B	98.8	86.4	92.3	79.4	92.1	77.2	88.7
UI-R1-E	99.6	80.1	95.6	75.4	91.6	81.2	88.7
UI-TARS-2B	95.2	79.1	90.7	68.6	87.2	78.3	84.7
UI-TARS-7B	96.9	<u>89.1</u>	<u>95.4</u>	<u>85.0</u>	<u>93.6</u>	<u>85.2</u>	<u>91.6</u>
UI-TARS-72B	94.8	86.3	91.2	87.9	91.5	87.7	90.3
UI-AGILE-3B	<u>99.6</u>	86.4	93.9	74.5	91.8	77.6	88.6
UI-AGILE-7B	100.0	91.1	95.6	84.8	94.2	83.0	92.1

Table 2: Grounding accuracy on ScreenSpot-v2. Results marked in bold represent the best performance, and underlined results indicate the second-best performance.

Models	AndroidControl-Low			AndroidControl-High		
	Type	GR	SR	Type	GR	SR
Os-Atlas-4B	64.6	71.2	40.6	49.0	49.5	22.8
Os-Atlas-7B	73.0	73.4	50.9	57.4	54.9	29.8
Qwen2.5-VL-3B	80.5	79.4	67.8	64.4	46.1	44.4
Qwen2.5-VL-7B	78.0	87.1	68.7	69.1	59.1	50.1
UI-R1-E	<u>87.0</u>	77.8	71.4	66.4	37.8	36.9
GUI-R1-3B	83.7	81.6	64.4	58.0	56.2	46.5
GUI-R1-7B	85.2	84.0	66.5	71.6	65.6	51.7
UI-AGILE-3B	85.4	<u>87.6</u>	<u>74.3</u>	<u>78.6</u>	60.7	<u>56.9</u>
UI-AGILE-7B	87.7	88.1	77.6	80.1	<u>61.9</u>	60.6

Table 3: Type, GR and SR on AndroidControl-Low and AndroidControl-High. Results marked in bold represent the best performance, and underlined results indicate the second-best performance.

also translate effectively to better decision-making and execution in complex, multi-step agent scenarios.

4.4 Ablation Study

To verify the contribution of each training technique, we conduct an ablation study of UI-AGILE-3B and the results are shown in Fig. 3(a) and Fig. 3(b). Due to page limit, the performance on AndroidControl w.r.t. Type and GR are provided in Appendix C. We can observe that:

- Applying continuous grounding reward and cropping-based resampling improves the performance by 10% and 12.4% on ScreenSpot-Pro, respectively. The former incentivizes more precise localization to the target’s center and the later helps avoid ineffective training with zero reward. They also slightly improve grounding accuracy on ScreenSpot-v2 where the performance of base model is already high and it is difficult to achieve significant gains.
- Removing “Simple Thinking” during training (i.e., “No

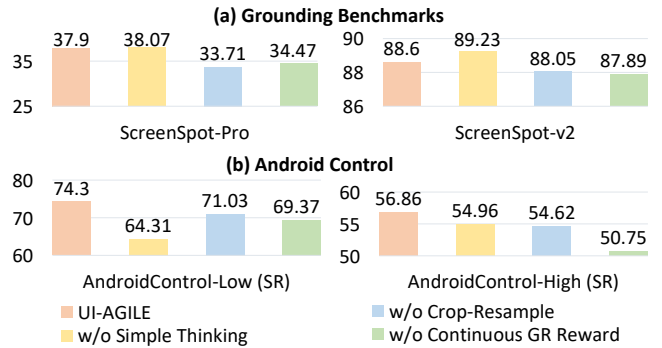


Figure 3: Ablation study.

Thinking”) leads to higher grounding accuracy on ScreenSpot-Pro and ScreenSpot-v2 (0.4% and 0.7% gains). However, Fig. 3(b) shows that integrating “Simple Thinking” enhances the agent’s decision-making with planning, resulting in a noticeable improvement in SR on AndroidControl, with SR increases of 15.5% and 3.4% in Low and High settings, respectively.

4.5 Analysis of Inference Time

We report the inference time of our decomposed grounding with selection method on the full ScreenSpot-Pro dataset (Li et al. 2025) using the vLLM framework (Kwon et al. 2023) and one 80G A800 GPU card.

As a baseline, the standard grounding approach applied to UI-AGILE-7B completes the benchmark in **30 minutes**. When applying our method, the decomposed grounding stage takes **35 minutes**. The subsequent VLM-based selection stage requires additional **4 minutes**. The modest increase in overhead is a practical trade-off for the substantial gain of grounding accuracy brought by our method.

4.6 Analysis of Attempts Per Step

Due to space limit, we include the analysis of attempts per training step in Appendix D.

5 Conclusions

In this paper, we introduce UI-AGILE, a comprehensive framework designed to enhance GUI agents’ training and inference. It tackles the practical challenges of the reasoning-grounding dilemma, ineffective reward, and visual noise. Experimental results demonstrate the effectiveness of our proposed techniques on enhancing GUI agents’ grounding capability and general capability.

Despite the promising performance of UI-AGILE, the VLM used in its decomposed grounding with selection method is a general-purpose, pre-trained model that is not originally tuned for the selection task. A promising future direction would be to fine-tune this adjudicator model on a curated dataset of candidate UI elements, enhancing its selection accuracy to achieve further gains in overall grounding performance.

References

- Bai, S.; Chen, K.; Liu, X.; Wang, J.; and et al, W. G. 2025. Qwen2.5-VL Technical Report. arXiv:2502.13923.
- Bengio, Y.; Louradour, J.; Collobert, R.; and Weston, J. 2009. Curriculum learning. In *ICML*, volume 382, 41–48.
- Chen, L.; Li, L.; Zhao, H.; Song, Y.; and Vinci. 2025. R1-V: Reinforcing Super Generalization Ability in Vision-Language Models with Less Than \$3. <https://github.com/Deep-Agent/R1-V>. Accessed: 2025-02-02.
- Chen, Z.; Luo, X.; and Li, D. 2025. VisRL: Intention-Driven Visual Perception via Reinforced Reasoning. arXiv:2503.07523.
- Cheng, K.; Sun, Q.; Chu, Y.; Xu, F.; Li, Y.; Zhang, J.; and Wu, Z. 2024. SeeClick: Harnessing GUI Grounding for Advanced Visual GUI Agents. In *ACL*, volume 1, 9313–9332.
- DeepSeek-AI; Guo, D.; Yang, D.; Zhang, H.; Song, J.; and et al, R. Z. 2025. DeepSeek-R1: Incentivizing Reasoning Capability in LLMs via Reinforcement Learning. arXiv:2501.12948.
- Gou, B.; Wang, R.; Zheng, B.; Xie, Y.; Chang, C.; Shu, Y.; Sun, H.; and Su, Y. 2025. Navigating the Digital World as Humans Do: Universal Visual Grounding for GUI Agents. In *ICLR*.
- Hong, W.; Wang, W.; Lv, Q.; Xu, J.; Yu, W.; Ji, J.; Wang, Y.; Wang, Z.; Dong, Y.; Ding, M.; and Tang, J. 2024. CogAgent: A Visual Language Model for GUI Agents. In *CVPR*, 14281–14290.
- Jaech, A.; Kalai, A.; Lerer, A.; Richardson, A.; and et al, A. E. 2024. OpenAI o1 System Card. arXiv:2412.16720.
- Kwon, W.; Li, Z.; Zhuang, S.; Sheng, Y.; Zheng, L.; Yu, C. H.; Gonzalez, J.; Zhang, H.; and Stoica, I. 2023. Efficient Memory Management for Large Language Model Serving with PagedAttention. In *SOSP*, 611–626.
- Li, J.; and Huang, K. 2025. A Summary on GUI Agents with Foundation Models Enhanced by Reinforcement Learning. arXiv:2504.20464.
- Li, K.; Meng, Z.; Lin, H.; Luo, Z.; Tian, Y.; Ma, J.; Huang, Z.; and Chua, T. 2025. ScreenSpot-Pro: GUI Grounding for Professional High-Resolution Computer Use. arXiv:2504.07981.
- Li, W.; Bishop, W. E.; Li, A.; Rawles, C.; Campbell-Ajala, F.; Tyamagundlu, D.; and Riva, O. 2024. On the Effects of Data Scale on UI Control Agents. In *NeurIPS*.
- Lin, K. Q.; Li, L.; Gao, D.; Yang, Z.; Wu, S.; Bai, Z.; Lei, S. W.; Wang, L.; and Shou, M. Z. 2025. ShowUI: One Vision-Language-Action Model for GUI Visual Agent. In *CVPR*, 19498–19508.
- Liu, Y.; Li, P.; Xie, C.; Hu, X.; Han, X.; Zhang, S.; Yang, H.; and Wu, F. 2025a. InfiGUI-R1: Advancing Multimodal GUI Agents from Reactive Actors to Deliberative Reasoners. arXiv:2504.14239.
- Liu, Z.; Sun, Z.; Zang, Y.; Dong, X.; Cao, Y.; Duan, H.; Lin, D.; and Wang, J. 2025b. Visual-RFT: Visual Reinforcement Fine-Tuning. arXiv:2503.01785.
- Lu, Z.; Chai, Y.; Guo, Y.; Yin, X.; Liu, L.; Wang, H.; Xiong, G.; and Li, H. 2025. UI-R1: Enhancing Action Prediction of GUI Agents by Reinforcement Learning. arXiv:2503.21620.
- Luo, R.; Wang, L.; He, W.; and Xia, X. 2025. GUI-R1 : A Generalist R1-Style Vision-Language Action Model For GUI Agents. arXiv:2504.10458.
- Meng, F.; Du, L.; Liu, Z.; Zhou, Z.; Lu, Q.; Fu, D.; Shi, B.; Wang, W.; He, J.; Zhang, K.; Luo, P.; Qiao, Y.; Zhang, Q.; and Shao, W. 2025. MM-Eureka: Exploring Visual Aha Moment with Rule-based Large-scale Reinforcement Learning. arXiv:2503.07365.
- Peng, Y.; Zhang, G.; Zhang, M.; You, Z.; Liu, J.; Zhu, Q.; Yang, K.; Xu, X.; Geng, X.; and Yang, X. 2025. LMM-R1: Empowering 3B LMMs with Strong Reasoning Abilities Through Two-Stage Rule-Based RL. arXiv:2503.07536.
- Qin, Y.; Ye, Y.; Fang, J.; and et al, H. W. 2025. UI-TARS: Pioneering Automated GUI Interaction with Native Agents. arXiv:2501.12326.
- Rafailov, R.; Sharma, A.; Mitchell, E.; Manning, C. D.; Ermon, S.; and Finn, C. 2023. Direct Preference Optimization: Your Language Model is Secretly a Reward Model. In *NeurIPS*.
- Schulman, J.; Wolski, F.; Dhariwal, P.; Radford, A.; and Klimov, O. 2017. Proximal Policy Optimization Algorithms. arXiv:1707.06347.
- Shao, Z.; Wang, P.; Zhu, Q.; Xu, R.; Song, J.; Zhang, M.; Li, Y. K.; Wu, Y.; and Guo, D. 2024. DeepSeekMath: Pushing the Limits of Mathematical Reasoning in Open Language Models. arXiv:2402.03300.
- Shen, Y.; Zhang, J.; Huang, J.; Shi, S.; Zhang, W.; Yan, J.; Wang, N.; Wang, K.; and Lian, S. 2025. DAST: Difficulty-Adaptive Slow-Thinking for Large Reasoning Models. arXiv:2503.04472.
- Vaswani, A.; Shazeer, N.; Parmar, N.; Uszkoreit, J.; Jones, L.; Gomez, A. N.; Kaiser, L.; and Polosukhin, I. 2017. Attention is All you Need. In *NIPS*, 5998–6008.
- Wan, J.; Song, S.; Yu, W.; Liu, Y.; Cheng, W.; Huang, F.; Bai, X.; Yao, C.; and Yang, Z. 2024. OMNIPARSER: A Unified Framework for Text Spotting, Key Information Extraction and Table Recognition. In *CVPR*, 15641–15653.
- Wang, S.; Liu, W.; Chen, J.; Gan, W.; Zeng, X.; Yu, S.; Hao, X.; Shao, K.; Wang, Y.; and Tang, R. 2024. GUI Agents with Foundation Models: A Comprehensive Survey. arXiv:2411.04890.
- Wu, Z.; Wu, Z.; Xu, F.; Wang, Y.; Sun, Q.; Jia, C.; Cheng, K.; Ding, Z.; Chen, L.; Liang, P. P.; and Qiao, Y. 2025. OS-ATLAS: Foundation Action Model for Generalist GUI Agents. In *ICLR*.
- Xie, T.; Deng, J.; Li, X.; Yang, J.; and et al, H. W. 2025. Scaling Computer-Use Grounding via User Interface Decomposition and Synthesis. arXiv:2505.13227.
- Xu, Y.; Wang, Z.; Wang, J.; Lu, D.; Xie, T.; Saha, A.; Sahoo, D.; Yu, T.; and Xiong, C. 2024. Aguviz: Unified Pure Vision Agents for Autonomous GUI Interaction. arXiv:2412.04454.

Yang, Y.; Li, D.; Yang, Y.; and et al, Z. L. 2025. GRPO for GUI Grounding Done Right. <https://huggingface.co/blog/HelloKKMe/grounding-r1>. Accessed: 2025-06-13.

Yang, Y.; Wang, Y.; Li, D.; Luo, Z.; Chen, B.; Huang, C.; and Li, J. 2024. Aria-UI: Visual Grounding for GUI Instructions. arXiv:2412.16256.

Zhang, C.; He, S.; Qian, J.; Li, B.; Li, L.; Qin, S.; Kang, Y.; Ma, M.; Liu, G.; Lin, Q.; Rajmohan, S.; Zhang, D.; and Zhang, Q. 2025. Large Language Model-Brained GUI Agents: A Survey. *Trans. Mach. Learn. Res.*, 2025.

Zhou, Y.; Dai, S.; Wang, S.; Zhou, K.; Jia, Q.; and Xu, J. 2025. GUI-G1: Understanding R1-Zero-Like Training for Visual Grounding in GUI Agents. arXiv:2505.15810.

A Environment and Implementation Details

In the following, we provide the details of experiment environment and our implementation.

Experiment Environment. We use a machine with two Intel(R) Xeon(R) Silver 4314 CPU @ 2.40GHz, 128GB main memory and eight NVIDIA A800 GPU for experiments.

Training Details. We use the trl framework to implement the cropping-based resampling strategy and reward functions. The sampling process is attempted 4 times at most and is bypassed entirely if the bbox’s dimensions exceed the target crop size. Following prior works, we use Qwen2.5-VL-3B and Qwen2.5-VL-7B as base models.

Inference Details. For decomposed grounding with selection, the input image is divided into four sub-images scaling to 60% of the original dimensions, with adjacent sub-images overlapping by 10% of the original image’s width and height. In the element image extraction stage, we define the element’s area by creating a simple bounding box centered on the predicted point with the width and height equal to 14% of the sub-image’s width and height. We have also explored a more sophisticated approach using OmniParser to refine this bounding box. However, it does not improve performance and increases the inference overhead. In the selection stage, we use Qwen2.5VL-7B-instruct to choose the final answer and the prompt is listed in Fig. 4.

Default Hyperparameters. Tab. 4 provides the default hyperparameters of UI-AGILE where cropping factor is the width and height ratio of new attempted image and last attempted image.

Hyperparameter	Value
learning rate	from 1e-06 to 4.36e-10
num generations	8
num train epochs	2
per device train batch size	4
cropping factor	0.6
gradient accumulation steps	4

Table 4: Default Hyperparameters

B Code

We provide the code for our RFT training and the Decomposed Grounding with Selection method in two separate modules. To avoid potential dependency conflicts, each module is designed to be run in its own conda environment.

To ensure a fair and comprehensive comparison, we conducted extensive experiments on the ScreenSpot-Pro benchmark. This involved re-implementing baseline models and evaluating them with our Decomposed Grounding with Selection method.

We use the parquet format to store test data in order to reduce the I/O read overhead.

We still have room for improvement in the implementation of Decomposed Grounding with Selection for Inference, including multi-threading to accelerate processing images and other non-GPU operations.

Prompt for VLM-based Adjudication

Instruction: {instruction content}.

Question: Does this image accurately match the instruction? Yes or No?

Answer:

Figure 4: Prompt for VLM-based adjudication.

C Ablation Study

Fig 5 provides results of the ablation study using Type and GR as evaluation metrics on AndroidControl. We can observe that each component in UI-AGILE indeed contributes to the overall performance.

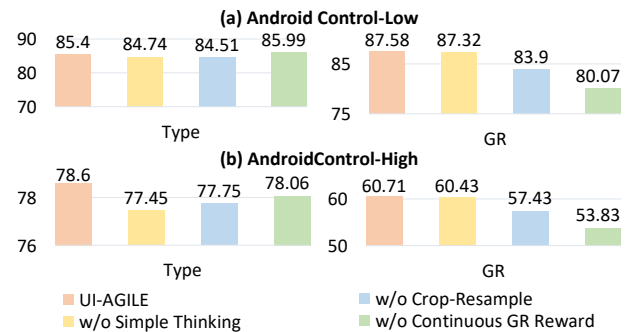


Figure 5: Ablation study using Type and GR as evaluation metrics on AndroidControl.

D Analysis of Attempts Per Step

Fig. 6 shows the distribution of attempts per GRPO training step, where each step processes a batch of two training samples. In the first epoch, we find that only 61.8% of training steps are fully successful on the initial attempt (i.e., both samples in the batch are solved without resampling). This means that without our strategy, a minimum of 19.1%

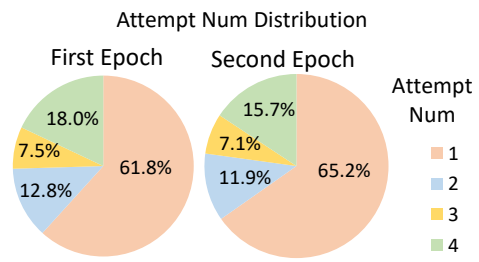


Figure 6: Distribution of attempts per step throughout the training process. Max attempt number is set to 4.

(38.2% ÷ 2) of training samples would have provided no learning signal. Overall attempt numbers decreases in the second epoch, demonstrating that the model learns from the samples salvaged by our method.